

Future scenarios of air temperature maximums and minimums for Georgia based on statistical downscaling

T. Davitashvili^a, L. Megrelidze^b, R. Kvatadze^c, I. Samkharadze^d,
G. Gogichaishvili^b, N. Kutaladze^{b*}, G. Mikuchadze^c

^aIlia Vekua Institute of Applied Mathematics of Ivane Javakhishvili Tbilisi State University, 2, University Str., Tbilisi, 0186, Georgia

^bThe Ministry of Environmental Protection and Agriculture of Georgia, National Environmental Agency, 150, David Agmashenebeli Ave., Tbilisi, 0012, Georgia

^cGeorgian Research and Educational Networking Association GRENA, 10 Chovelidze Street, Tbilisi, 0108, Georgia

^dIvane Javakhishvili Tbilisi State University, 1, Chavchavadze Ave., Tbilisi, 0179, Georgia

Received: 14 March 2020; accepted: 19 May 2020

ABSTRACT

In this article monthly maximums and minimums of 2-meter air temperature from three GCMs of CMIP5 [1] database has been statistically downscaled using RCMES [2] package, with four different methods for 27 selected meteorological stations on the territory of Georgia. Stations have been selected all over the territory of Georgia, based on the completeness of their air temperature series throughout the entire period of 1961–2010, their credibility (measured by the number of non-missing data) and to cover as much complex climate features of the territory as possible. The downscaling methods have been trained for the period of 1961–1985 and validated for the period of 1986–2010. Some statistical parameters have been calculated by applying R statistics environment to compare observed and simulated time series and to evaluate temporal and spatial goodness of each method. Downscaling model, driven by the validation study was used for future T_{min} and T_{max} time series construction for the 2021–2070 period under RCP4.5 and RCP8.5 scenarios. Temperatures time series have been constructed from a multimodel ensemble, with mean and spread. Future change tendencies have been assessed in comparison of the period of 1986–2010 but was also compared with previous 25-years period (1961–1985) to compare future changes with the magnitudes of past tendencies.

Keywords: Statistical downscaling, GCM, Regression, Bias correction, Future projection, Multi-model ensemble.

*Corresponding author: Nato Kutaladze; E-mail address: cwlam08@gmail.com

Introduction

The climate change signal is not uniform over the globe, contrary to long-term trends and year-to-year variability of the mean meteorological variables and especially extremes considerably varies for different geographical regions [3]. The Global Climate Models (GCMs), or also referred as the General Circulation Models demonstrate a significant skill to simulate climate change information at the continental and hemispheric spatial scales and incorporate a large proportion of the complexity of the global system, but they are far from being per-

fect even at a global scale. Future climate change information is uncertain due to mentioned complexity and inadequacy of the models in capturing all of its underlying processes, also for unknown amount of future emission and climate internal variability. Careful and systematic evaluation of GCMs from multiple climate modeling centers is widely recognized as critical for improving our understanding of future climate change. The Coupled Model Inter-comparison Project (CMIP), currently in its sixth phase, is an internationally coordinated multi-GCM experiment that has been undertaken for decades to assess global-scale climate change [4–5].

It should be noted that characterizing present climate conditions and providing future climate projections at a regional scale is an extremely difficult task [6] (Mahmood and Babel 2013) as it involves additional uncertainties while reducing, a spatial scale of GCMs simulated climate parameters. GCMs have a very coarse spatial resolution and are unable to simulate sub-grid scale features and physical dynamics [7] and outputs are often too coarse to be effectively used in climate change impacts, adaptation, and vulnerability assessment studies [8]. The decrease in spatial accuracy of GCMs simulated climate variables occurs from continental to local scale using statistical downscaling (SD) or dynamical downscaling (DD) techniques. The last option involves the use of high-resolution Regional Climate Model (RCM) to simulate physical processes at fine spatial scale from the host GCM and is considered as costly and time-consuming one [9-11] (Giorgi 1990; Jones et al. 1995). SD is faster and simpler in use, less computationally expensive and applicable for uncertainty and risk analyses [12].

Using SD a statistical/empirical relationship is established between GCMs simulated large-scale atmospheric variables (predictors) with station (local) scale meteorological variables (predictands) [13-15] A Statistical downscaling method by itself divides into three groups: multiple linear regression, nonlinear regression (e.g. artificial neural networks) and stochastic weather generators, which mostly are used in different sectoral impact studies. Each SD method includes the uncertainties in downscaling result from the concept on which the downscaling models are based and from the data used in the study.

The variability of the results obtained using different types of downscaling models suggest the use of as many statistical downscaling methods as possible in the development of climate change projections at the local scale. These capabilities are necessary to ensure reliable characterization of the future climate, which can lead to conscious decision-making, taking into account the climate characteristics of the region.

There are several studies devoted to the regional climate change projection for Georgia and more widely, for the South Caucasus region. These studies are mostly focused on regional climate modeling approaches and describe how well the regional climate models (RCMs) simulate regional and local climate peculiarities. Mainly two GCMs are mentioned in above-mentioned researches dynamically downscaled by also two different RCMs. Some seldom researches are also available, in which fu-

ture climate change patterns for Georgia is assessed based on GCM ensemble. There is a gap in studies specifically focused on assessing uncertainty in downscaling results due to different statistical methods, also in a creation of ensembles from different GCMs and SD methods on several sites on the territory of Georgia [16-17].

We have performed statistical downscaling using RCMES - Regional Climate Model Evaluation System (RCMES) package. Mean monthly maximums and minimums of 2-meter air temperature from 3 GCMs of CMIP5 database with four different methods have been downscaled for 27 locations, where Georgian hydro-meteorological stations are located. Models based on SD methods have been trained for the period of 1961-85 and validated for the period of 1986-2010. Different statistical metrics were used to assess models performance, beyond of means and variances comparison. Results of this study discussed and Representative Concentration Pathway (RCP 4.5, RCP 8.5) scenarios constructed for above-mentioned 27 locations in chapter 2.

1. Data and method

1.1. Study area

Georgia's climate conditions are very diverse for a relatively small territory of the country, that is a result of its location on the northern edge of the subtropical zone between the Black and Caspian seas and also because of the complexity of its special topography. Climatic peculiarities in Georgia are mostly conditioned by the Greater Caucasus mountain range from the north and to the Black Sea in the west. The Greater Caucasus range serves as a barrier against cold air from the north. Warm, moist air from the Black Sea easily moves into the coastal lowlands from the west. Climatic zones are determined by a distance from the Black Sea and by the altitude. The Lesser Caucasus range runs parallel to the Turkish and summers and cold winters. Precipitation is comparatively less than at the same heights elsewhere in Georgia.

In the Fig. A.1 maps of annual mean maximal and minimal temperatures averaged over 1961-85 period are presented, where 27 stations of Georgian meteorological network are also marked. Time series from these stations of temperature mean monthly maximums and minimums have been used for this study. Selection criteria of these stations with some additional information is provided below in section 3.1.

1.2. RCMES toolkit

We decided to choose RCMES for performing our study. The Regional Climate Model Evaluation System (RCMES) is an enabling tool of the National Aeronautics and Space Administration to support the United States National Climate Assessment [2]. RCMES is designed to yield information from the various database to import climate models and observations in different formats, also performance metrics are designed to assess and quantify model skill, with plotting and visualization routines. Besides of above-mentioned user-friendly interfaces for quickly configuring is an additional benefit.

RCMES is an open, publicly accessible process enabled by leveraging the Apache Software Foundation's OSS library, Apache Open Climate Workbench (OCW). RCMES provides datasets and tools to assess the quantitative strengths and weakness of climate models, typically under present climate conditions for which we have observations for comparison, which then forms a basis to quantify our understanding of model uncertainties in future projections. OCW also allows users to build their own climate data analysis tools, such as the statistical downscaling toolkit provided as a part of RCMES.

We performed statistical downscaling using RCMES package for near-surface mean maximum and minimum temperature from 3 GCMs - MPI-ESM-MR; HadGEM2-ES; GFDL-CM3 runs existing in CMIP5 database and available via RCMES.

1.3. GCM data (Baseline and Future scenarios)

RCMES toolkit allowing direct access to CMIP (e.g. CMIP5, CMIP6) global models, through access to the Earth System Grid Federation. Coupled Model Inter-comparison Project (CMIP) was established under the World Climate Research Programme (WCRP) by Working Group on Coupled Modelling (WGCM) as a standard experimental protocol for studying the output of coupled atmosphere-ocean general circulation models (AOGCMs). CMIP provides a community-based infrastructure in support of climate model diagnosis, validation, inter-comparison, documentation and data access [18-21]. The Output from about 60 GCMs with various historical experiment simulations and future emission scenarios are available on this database. We downscaled output temperatures from only three of them. GCM selection criteria was meant to use those models where we plan to have or

already got dynamically downscaled results.

Below in the table B.1. Grid Resolutions of selected three GCMs - namely for atmosphere and ocean are presented.

Table B 1. *Grid Resolutions of selected three GCMs for atmosphere and ocean*

| Model | Atmospheric Grid | | Ocean Grid | |
|----------|------------------|-----------|------------------------|-----------|
| | Latitude | Longitude | Latitude | Longitude |
| GFDL-CM3 | 2 | 2,5 | 0,3344,1 | 1 |
| HadGEM2- | 1,25 | 1.875 | 0,3396 | 1 |
| MPI-ESM- | 1,875 | 1,875 | Orthogonal curvilinear | |

The climate model of the Geophysical Fluid Dynamics Laboratory's (GFDL) at NOAA is one of the leading climate models used in the Fifth Assessment Report of the IPCC. It encompasses the predictability and sensitivity of global and regional climate, the structure, variability, dynamics and interaction of the atmosphere and the ocean; and is influenced by various trace constituents. In CMIP5 phase of the project, version 3 of the model is participating. CM3 includes aerosol-cloud and chemistry-climate interactions, and links between the troposphere and stratosphere [22].

CMIP5 set of centennial experiments includes Met Office Hadley Centre's Earth System Model (ESM) HadGEM2-ES which focuses on how the climate system is likely to respond to human-induced disturbances. Model simulations consider greenhouse gas concentrations, aerosol precursors, stratospheric and tropospheric ozone assumptions, as well as an implementation of land-use change and natural forcings for the HadGEM2-ES historical and future experiments following the Representative Concentration Pathways [23].

The new Max-Planck-Institute Earth System Model (MPI-ESM) is used in the Coupled Model Inter-comparison Project phase 5 (CMIP5) in a series of climate change experiments for either idealized CO₂-only forcing or forcings based on observations and the Representative Concentration Pathway (RCP) scenarios. MPI-ESM (MPG) is a comprehensive Earth-System Model, in the sense that it consists of component models for the ocean, the atmosphere and the land surface. These components are coupled through the exchange of energy, momentum, water and important trace gases such as carbon dioxide [24].

On the upper panel of the Fig. A.2 maps of the T_{max} for 1961-85 period are presented. The first plot is constructed from CRU data, the second – from the output of GFDL-CM3, III and IV – from HadGEM2-ES and MPI-ESM-MR, respectively. On the second panel identical maps for T_{min} are presented.

1.4. The downscaling methods

Statistical downscaling involves the establishment of empirical relationships between historical and/or current large-scale atmospheric and local climate variables. Once relationships are defined and validated, atmospheric variables are used to predict future local climate variables. However, this approach relies on the critical assumption that the relationship between present large-scale circulation and local climate remains valid under different forcing conditions for future climate [25]. Main disadvantages of this method are: 1) local, small-scale dynamics and climate feedbacks are not simulated, as the GCMs are not able to simulate weather and climate processes at scales smaller than their grid spacing, and statistically downscaled data do not add information at the smaller scale, and 2) assumptions of stationarity between the large and small-scale dynamics are made to downscale future projections. The problem of assuming stationarity is that some of the interactions between the large and small-scale are already changing, so this information is not represented in the downscaled projections.

We Downscaled temperatures from 3 GCMs output with 4 different methods: Delta method (addition); Delta method (bias correction); Quantile mapping; Asynchronous linear regression.

1. Delta method (addition) is the technique, where the difference between present and future simulations are added to the present observation. First, the mean difference between present simulation and future simulation is calculated. The calculated difference is added to the present observation to make a downscaled future prediction. In this method, only the change in mean values in simulations is considered in the future projection and the variance remains unchanged [26]. Distribution of observed and raw Tmin time series from MPI-EMS-MR3 model output for trained (1961-85) and testing/validation periods (1986-2010) for Tbilisi are presented on the Fig. A.3 (a), and Fig. A.3 (b), the bottom plot represents distribution of a downscaled Tmin simulated by MPI-EMS-MR3 model for testing/validation period (1986-2010) for Tbilisi.

2. In Delta method (bias correction), the mean bias of present simulation from present observation is calculated and added to the future simulation [27]. Delta method uses a raw model output for the future period and corrects it using the differences (Δ) between historical reference data from the model and observations. If we assume the variability as equal

for both GCMs and observations, the monthly data is simply shifted by the mean bias in the reference period. On the Fig. A.4 (a) results of using bias correction method for the same time series are presented.

3. The other methodology is quartile mapping method fitting cumulative distribution functions of observed, training and testing data [28] Li et al. (2010). Quantiles for observed (XO), as well as GCM (XGCM) simulated data are first calculated. Then linear transformation to each quantile from GCM data to adjust its range is applied to match the quantile with observed data. The Same correction to the quantiles in the future data should be used. Downscaling results using quartile mapping method are shown on the Fig. A.4 (b).

4. Statistical Asynchronous Regression (SAR) method is a technique for determining a relationship between two-time varying quantities without simultaneous measurements of both quantities [29]. It requires that there is a time invariant, monotonic function $Y = u(X)$ relation between the two quantities, Y and X. In order to determine $u(X)$, we only need to know the statistical distributions of X and Y. $u(X)$ converts the distribution of X into the distribution of Y, while conserving probability. Downscaling results using Statistical Asynchronous Regression method are shown on the Fig. A.4 (c).

In the next chapter goodness and weakness of each method is discussed and some metrics are analyzed to prove some conclusions.

2. Validation results and discussion

2.1. Performance of model downscaling and validation

Prior to future scenario construction, the results of the observed data of mean monthly maximum and minimum temperature are compared with the simulated data during the training and validation periods using some statistical parameters (metrics).

Twenty-seven sites broadly scattered throughout Georgia were selected based on the completeness of their temperature series throughout the entire period of 1961–2010 and their credibility measured by the number of non-missing data, as well as to cover as much complex climate features of the country as possible. The locations and summary information for the 27 stations selected are shown in Fig. A.1 and Table B.1, respectively.

The study carried out the downscaling process for every 27 stations feeding three GCMs outputs

using four downscaling methods, which produced 27*3*4 time series for each parameter, and the study then took the best matching method for constructing future climate scenarios.

The models were trained (downscaled) using observations of 25 years of data (1961–1985, termed the base period) and the remaining 25 years of data (1986–2010, termed the validation period), respectively.

Model evaluation has been performed using R-Instat - open source menu driven statistical software, powered by R - programming language and free software environment for statistical computing and graphics, supported by the R Foundation for Statistical Computing [30].

2.2. Indicators of performance assessment

The Pearson's correlation coefficients (CC) and plots of squared CC values contributed to the identification and selection of the most valuable methods for developing the downscaling model. Except the CC to evaluate the quality of the model predictions, following metrics were used as measures of the statistical agreement between the predicted values and observed data, including the mean bias, mean absolute error (MAE), the root mean square error (RMSE), as well mean (μ), median (Med), standard deviation (SD), median absolute deviation (MAD), coefficient of variation (CV) and standard error of mean (SE $_{\mu}$). They were calculated for all three models and four downscaling methods separately.

The value of CC is indicative of strength between observed and simulated values whereas mean bias, MAE and RMSE are used to determine the accuracy of the model. However, μ , median and SE $_{\mu}$ are exercised to test how well the model predicted the mean values, while SD, CV and MAD are used to investigate the variability of data simulated by the model.

The last Indicator, chosen as the criteria for evaluating the performance of downscaling methods, was the assessment of an effect of each downscaling method on trends in seasonal and annual mean minimum and maximum temperatures for the validation period in comparison with the behavior of observed data series temporal variability. Spearman's Rho rank correlation was used to determine the statistical significance of trends for maximum and minimum temperature on seasonal and annual timescales. This statistic is a non-parametric measure of correlation, adapted to data sets with strong autocorrelation (temperature). It makes no assumptions about the probability of the distribution of the

investigated data and it is less affected by outliers or by any form of data discontinuity [31]. The statistical significance was determined at the 95% confidential-ity level. The magnitude of the trend was calculated by the slopes of the linear trends using ordinary least square fitting and expressed in °C decade⁻¹.

2.3. Evaluation of downscaling methods

Table B.3(a) shows the mean CCs between modeled and observed minimum temperatures for 3 GCMs using 4 candidate methods during the validation period (1986-2010) for each season over all 27 stations and Table B.3(b) shows the same for maximum temperature. Seasons are defined as follows: as the following: winter-DJF (December–February), spring-MAM (March–May), summer-JJA (June–August) and autumn-SON (September–November).

Overall, it is evident that both the simulated maximum and minimum temperatures were closely consistent with observations. CC between simulated and observed temperature exceeded or equaled to 0.8 in the validation period. Also, it could be seen that the minimum temperature is modelled slightly better than the maximum. There are some differences in seasonal dependence. Namely, for both parameters, summer and autumn seasons have higher correlations with observed patterns. Regarding the advantages of the methods, delta addition (1) and delta correction (2) methods are the most satisfactory.

Results of comparison between observed and downscaled mean annual Tmax, Tmin in terms of statistical measures for validation period are given in Table B.4(a) and Table B.4(b).

Mean annual biases in validation were in the range of (+0.33)÷(+0.94)°C and (+0.50)÷(+1.04)°C for minimum and maximum temperature, respectively, with MAE about 1.5-2°C and RMSE 2-2.5°C. Different patterns of bias are observed in seasonal context. Both maximum and minimum temperature differences are similar across the seasons. The greatest positive deviations (3-4°C) were found in winter for absolute errors and spring - for mean bias (Fig. A.5). The closest Simulations to observation have been found out in summer season. Annual and seasonal biases indicate that, in average, simulations for both parameters are overestimated regarding observed values with slightly higher deviations for maximum temperature, cool biases were found mostly in summer in the range up to 2°C. All three metrics assessing the accuracy of the models have a strong seasonality among a majority of stations,

the relatively less effect they display among coastal stations while in both variables, the largest and most seasonally dependent bias magnitudes originate from a high-mountainous stations (Fig. A.6).

Comparison of downscaling methods with regard to model errors show an overall warm bias of the same magnitude similar for three (delta edition, delta correction, quantile mapping) methods deviations are higher for the last – regression-based approach. For MAE, and RMSE the less matching method is the delta correction, while three other methods have approximately same deviations in mean annual values.

Analysis of other statistical metrics used to test model on the prediction of mean values demonstrate the abilities of those statistical downscaling methods to reproduce mean minimum and maximum temperature (Fig. A.7). The differences between modeled and observed parameters are not significant, all within a range of $\pm 0.8^{\circ}\text{C}$, depending on the metric. For instance, SD and SE_{μ} are strongly depended on site elevation and three among four downscaling methods (except delta correction) can reproduce this feature properly, whilst the best simulation of a median is performed by delta correction method.

After model evaluation by statistical metrics linear trend analysis has been fulfilled, the magnitude of annual and seasonal linear trends for maximum and minimum temperature for the investigated period (1986–2010) are presented in Table B.5.

Based on observation data, investigated stations show a positive trend with medium significance for both parameters in all seasons except winter, with the highest magnitude in autumn. In winter most trends are not significant, herewith minimum temperature has mostly cooling tendency. Due to this, annual trends are positive for both parameters, but with higher fidelity for minimum temperature. However, the magnitude of the trend is lower than the one for maximum temperature ($+0.41^{\circ}\text{C decade}^{-1}$ for minimums and $+0.60^{\circ}\text{C decade}^{-1}$ for maximums). In addition, the increase in minimum temperature is enhanced at the coastal zone and the western part of the country.

Finally, the effect of each downscaling method on trends in seasonal and annual average minimum and maximum temperatures have been investigated. Analysis of modeled data changing behavior shows that annual pattern of trends are more or less well captured by all GCMs downscaled using three of four methods. The exception is a delta addition method that revealed not a steady but negative

annual trend for both parameters. Seasonal trends coincidence is relevant to annual. The exception is again the winter with the minimum cooling tendency repeated only by delta addition method.

Annual trends representing the tendency of changes via year-to-year variability is significantly reduced by the delta addition method. As in this case, the linear trend of observed temperatures for the testing period (1961–85) is repeated in corresponding downscaled parameters for the validation period and warming tendency is stronger in the validation period, than in the beginning for entire territory in average.

Investigation of model performance indicators (metrics) revealed no clear indication of the best downscaling method. First one (delta addition) more likely fit the observation, the other three methods show no fixed advantage. Statistical trends analysis revealed the weakness of the delta addition method. Comparison of linear trends magnitudes suggest that the most appropriate method for both parameters is delta correction as the best associated with observed trends pattern [32].

3. Projected changes for future climate scenarios

Future T_{min} and T_{max} time series were constructed for the period of 2021–2070 under RCP4.5 and RCP8.5 scenarios by RCMES. We used delta correction method to produce desired future scenarios with reference to the period of 1961–85, where relationship between large-scale predictors –GCMs output T_{min} and T_{max} and local scale variables (stations T_{min} and T_{max}) have been established and validated. In the following sections, temporal and spatial changes of mentioned two parameters, obtained from three downscaled GCM ensembles are described. Corresponding deltas between two future periods 2021–2045 and 1946–2017 in comparison with the 1986–2010 period are presented on charts and in tables. As well, future changes have been compared with the magnitude of past tendencies comparing the period of 1986–2010 to previous 25-year period (1961–1985).

3.1. Variation of seasonal air temperatures

Mean seasonal observed (1961–1985, 1986–2010) and projected (2021–2045, 2046–2070) minimum and maximum temperature in Georgia under the two scenarios are shown in the Fig. A.8. All

mean seasonal temperatures increase in the future 50 years under both scenarios.

Regarding seasonal pattern, for T_{min} and T_{max} the most significant increase in the past period occurring in summer, in the range of 0.6–0.7°C, is predicted to be shifted in winter during the whole future period under both scenarios becoming the summer as the least experiencing warming season throughout the year. Although for T_{max} at the end of the 2060s minimum increase in the range of 2°C is anticipated in spring. The highest increase in T_{min} and T_{max} , up to 5°C is expected in winter under RCP8.5 scenarios in 2046–2070.

Overall, past trends are sustained and will be enhanced in the future. The exception is T_{max} behavior in autumn, when no significant decrease (-0.13°C) is observed in the 2000s, will be reversed in future. According to simulation, autumn maximums will grow rapidly than in other seasons and will reach up to +3.96, and +4.58°C to the end of the 2060s under the RCP4.5, and RCP8.5 scenarios, respectively, that are the highest after winter positive increments in the range of +4.26, and +5.19°C. In the 2040s, the minimum increase under both scenarios for minimums is 0.14°C occurring in summer and for maximums is 0.41°C, occurring in spring, increasing to 1.5 and 2.5°C to the end of 2060s.

Therefore, the temperature will show an obviously increasing tendency averaged over entire territory in the future. The patterns of increase are similar for minimum and maximum temperatures with slightly more considerable warming for maximums than for minimums.

3.2. Variation of annual mean air temperatures

Fig. A.9 shows the projections obtained for minimum/maximum temperature averaged over the 27 stations of Table B.2. Different colors correspond to distinct scenarios. The solid lines correspond to the ensemble means for the RCP4.5 and RCP8.5 scenarios. The Spread of models are shown as shaded areas for each scenario and models historical run for 1961–2010 with observation time-series plotted as a black solid line. As can be seen all GSM/RCP project are increasing temperatures. For both temperature variables, the MPI-ESM-MR (GFDL-CM3) systematically projects the weakest (strongest) increments, whereas the HadGEM2 provides moderate results. The mean increments for 2021–2045 and 2046–2070 are in between 1.5°C and 4.5°C (2°C

and 5°C) for minimum (maximum) temperature, depending on the GCM and RCP.

Table B.6 shows the changes in temperature for Georgia in the 2000s, 2040s, and 2060s with respect to the reference period under the RCP4.5 and RCP8.5 scenarios obtained from the RCMES. Under the RCP4.5 scenario, the mean annual minimum (maximum) temperature will increase by 1.66 (1.91) and 2.62°C (3.14) in the 2040s, and 2060s, respectively that are significantly higher than the past 2000s increments (0.32°C) with regard to 1980s, for both targeted variables. As expected, the changes under RCP8.5 are greater than under RCP4.5 and mean annual minimum (maximum) temperature will increase by 1.82 (2.16) and 3.35°C (4.01) in the 2040s, and 2060s, respectively. Therefore, it is clear that in Georgia temperature shows significant positive trends and these changes will be more intensive towards the end of this century.

It is also revealed that increase in T_{max} is more prominent than in T_{min} . The upward rate of T_{max} is especially obvious under RCP8.5 for the second future period. Except this, the difference between two scenarios is also more considerable for T_{max} and for annual values, it is in the range of 0.7–0.9°C whilst for T_{min} it is not more than 0.2–0.3°C, depending on the period.

3.3 Spatial patterns of air temperature

In order to assess the spatial distribution of these results, deltas are calculated by subtracting the mean of the historical reference period (1986–2010) from the ensemble mean of the target scenario periods (2021–2045 and 2046–2070) - for all investigated stations over the country. Positive deltas are obtained throughout the whole country for both temperatures, finding the highest increments over the plain territory of east Georgia. Moreover, the projected warming signal is higher for minimum than for maximum temperature, extended also over the west Georgia central lowlands in the second future 25-years period. The smallest warming magnitudes are revealed in the Black Sea coastal zone and adjacent lowlands under both scenarios for the whole future period. Relatively moderate changes are expected in the high-mountainous area with the altitude higher 1000 and 1500 meter above sea level for minimum and maximum temperatures, respectively. Finally, the two RCPs considered lead to similar delta spatial patterns (although intensified for the RCP8.5) for the two target variables. It should

be noted that revealed spatial peculiarities of warming are in accordance with the past period, but with slightly greater magnitudes of upward trends for maximum temperature. Also, the most significant warming occurring currently in the furthest eastern part (Kakheti region) getting relatively less intensive in future with regard to the rest of the territory.

In the 2000s the spatial distribution of the increase in air temperature is similar for both variables experiencing greater warming in the east part of the country with the average magnitude not more than a half degree with regard 1980s records. Furthermore, the maximum warming is located over Kakheti region (East Georgia), reaching $+0.54^{\circ}\text{C}$.

For the 2040s, the experiencing warming is greater than in the 2000s and is mainly located over Qvemo Kartli region (East Georgia), where the annual minimum and maximum temperature will increase by amounts in the range $2.0\text{--}2.5^{\circ}\text{C}$ under both RCP4.5 and RCP8.5. The remaining parts experiencing slightly less warming ($1.5\text{--}2.0^{\circ}\text{C}$).

In the 2060s, the increase will be larger than 3°C in most of the territory under RCP8.5 and up to $4.0\text{--}4.5^{\circ}\text{C}$ under RCP4.5. In addition, the maximums increase will be greater than minimums.

On the whole, most of the territory may experience an obviously increasing trend in the future 50-years period under both scenarios. However, a few areas, including some patches, such as coastal zone and mountainous regions, are expected to show not so steady trends. With the passage of the decades (the 2000s, 2040s, and 2060s), the increase will be greater, and the area of higher temperature will grow in size.

4. Conclusion

Validation of statistical downscaling methods show that all of the methods have some advantages and disadvantages on the temporal and spatial scale. The metrics we used for model performance evaluation varies from station to station, year to year, and season to season.

The results of calculations have shown that the mean Person's CCs between modeled and observed Tmax and Tmin for all three GCMs (GFDL, MPI, HadGEM2) using four candidate methods for each season, over all 27 stations, exceeded or equaled to 0.8 during the validation period (1986–2010). Also, Tmin has been modelled slightly better than Tmax for both parameters, summer and autumn seasons have slightly higher correlations with observed pat-

terns and delta addition with delta correction method had the most satisfactory results.

Comparison of downscaling methods, with regard model errors, have shown an overall warm bias of the same magnitude similar for three (delta edition, delta correction, quantile mapping) methods and deviations have been higher for the last – regression-based approach. For MAE and RMSE the less matching method was the delta correction, while three other methods had approximately same deviations in mean annual values.

The magnitudes of annual and seasonal linear trends for Tmin and Tmax based on observation data in all seasons except winter (Tmin had mostly cooling tendency) were positive with medium significance (with the highest magnitude in autumn, with higher fidelity for Tmin) for the investigated period (1986–2010). However, the magnitude of the trend is lower for minimum compare to maximum temperature ($+0.41^{\circ}\text{C decade}^{-1}$ for minimums and $+0.60^{\circ}\text{C decade}^{-1}$ for maximums). In addition, the increase in minimum temperature is enhanced at the coastal zone and the western part of the country.

The effect of each downscaling method on the tendency of seasonal and annual average Tmin and Tmax has shown that annual pattern of trends more or less well captured by all downscaling methods with exception of delta addition method.

Investigation of model performance indicators (metrics) revealed no clear indication of the best downscaling method. Delta addition method more likely fit the observation, the other three methods show no fixed advantages. Statistical trends analysis revealed the weakness of the delta addition method. Comparison of linear trends magnitudes suggest that the most appropriate method for both parameter is delta correction as the best associated with observed trends pattern and future temperatures were downscaled using this method.

According to the simulations the mean annual minimum (maximum) temperature will increase by 1.66 (1.91) and 2.62°C (3.14) in the 2040s, and 2060s under the RCP4.5 scenario, that are significantly higher than the past 2000s increments (0.32°C) with regard to 1980s, for both targeted variables. As expected, the changes under RCP8.5 are greater than under RCP4.5 and mean annual minimum (maximum) temperature will increase by 1.82 (2.16) and 3.35°C (4.01) in the 2040s, and 2060s, respectively.

Regarding the seasonal pattern, for Tmin and Tmax past trends are sustained and will enhance in the future. The most significant increase is predict-

ed to be in winter during the whole future period under both scenarios becoming the summer as the least experiencing warming season throughout the year. Although for Tmax at the end of 2060s minimum increase in the range of 2°C anticipated in spring. The highest increase in Tmin and Tmax up to 5°C is expected in winter under RCP8.5 scenarios in the period of 2046-2070.

It should be noted that this research contains several uncertainties (choice of GCM, RCP and downscaling methods) and more precise investigations of each type of uncertainties and calculation of probabilities are planned for the future.

Acknowledgement

The research was funded by the Shota Rustaveli National Science Foundation of Georgia Grant N FR17_548.

Reference

- [1] <https://esgf-node.llnl.gov/projects/cmip5/>
- [2] <https://rcmes.jpl.nasa.gov/>
- [3] J. Cortereal, X. B. Zhang, and X. L. Wang, Downscaling GCM information to regional scales – a nonparametric multivariate regression approach, *Clim Dynam*, 11 (7) (1995) 413-424.
- [4] T. F. Stocker, *Climate Change 2013: The Physical Science Basis: Working Group I Contribution to the Fifth Assessment Report of the Intergovernmental Panel on Climate Change*, Cambridge University Press, 2014.
- [5] IPCC, *Summary for Policymakers//Climate Change 2013: The Physical Science Basis. Contribution of Working Group I to the Fifth Assessment Report of the Intergovernmental Panel on Climate Change*, Cambridge University Press, 2013.
- [6] R. Mahmood and M.S. Babel, Evaluation of SDSM Developed by Annual and Monthly Sub-Models for Downscaling Temperature and Precipitation in the Jhelum Basin, Pakistan and India. *Theoretical and Applied Climatology* 113 (2012) 27-44. <http://dx.doi.org/10.1007/s00704-012-0765-0>
- [7] B.C. Hewitson, and R.G. Crane, Climate downscaling: Techniques and applications, *Clim. Res.*, 7 (1996) 85-95.
- [8] L.E. Hay, R.L. Wilby, and G.H. Leagesley, A comparison of delta change and downscaled GCM scenarios for three mountainous basins in the United States. *Journal of the American Water Resources Association*, 36 (2000) 387-397.
- [9] F. Giorgi, Simulation of regional climate using a limited area model nested in a general circulation model. *J. Climate* 3 (1990) 941-963.
- [10] F. Giorgi and L.O. Mearns, Approaches to the simulation of regional climate change: a review. *Rev. Geophys.* 29 (1991) 191-216.
- [11] F. Giorgi and L.O. Mearns, Regional climate modelling revisited. An introduction to the special issue. *J. Geophys. Res.* (1999) 104 6335-6352.
- [12] B. C. Hewitson, and R. G. Crane, Global climate change: Question of downscaled climate scenarios for impact assessment. *Bulletin of the American Meteorological Society* (submitted) (2004).
- [13] L. O. Mearns, C. Rosenzweig, and R. Goldberg, Mean and variance change in climate scenarios: Methods, agricultural applications, and measures of uncertainty. *Climatic Chang*, 35 (1997) 367-396.
- [14] J.M. Murphy, Predictions of climate change over Europe using statistical and dynamical downscaling techniques. *Int. J. Climatology*, 20, (2000)489-501.
- [15] M. New, M. Hulme and P.D. Jones, Representing twentieth century space-time climate variability. Part 1: development of a 1961-90 mean monthly terrestrial climatology. *J. Climate*, 12 (1999) 829-856.
- [16] M.Elizbarashvili, E.Elizbarashvili, N.Kutaladze, Sh.Elizbarashvili, R.Maisuradze, T. Eradze, N, Jamaspashvili, N. Gogia, *Climatology and Historical Trends in Tropical Nights over the Georgian Territory. Earth Sciences. Special Issue: New Challenge for Geography: Landscape Dimensions of Sustainable Development. Vol. 6, No. 5-1 (2017) 23-30. doi: 10.11648/j.earth.s.2017060501.14*
- [17] T. Davitashvili, N. Kutaladze, R. Kvatadze and G. Mikuchadze (2018). Effect of dust aerosols in forming the regional climate of Georgia. *Scalable Computing: Practice and Experience*, 2018, Volume 19, Number 2, pp. 199–208.
- [18] R.L. Wilby, T.M.L. Wigley, D. Conway, P.D. Jones, Hewitson, B.C., Main, J. and D.S. Wilks, Statistical downscaling of general circulation model output: a comparison of methods. *Water Resources Research*, 34 (1998)

2995-3008.

- [19] D.I. Jeong, A. St-Hilaire, TBMJ. Ouarda, P. Gachon, CGCM3 predictors used for daily temperature and precipitation downscaling in Southern Quebec, Canada. *Theoretical and Applied Climatology* 107 (2012) 389–406. DOI: 10.1007/s00704-011-0490-0.
- [20] R. Knutti, R. Furrer, C. Tebaldi, J. Cermak, G.A. Meehl, Challenges in combining projections from multiple climate models. *Journal of Climate* 23 (2010) 2739–2758. DOI: 10.1175/2009JCLI3361.1.
- [21] A. W. Wood, L. R. Leung, V. Sridhar, and D. P. Lettenmaier, Hydrologic implications of dynamical and statistical downscaling approaches to downscaling climate model outputs. *Climatic Change* (to appear, 2004) (2004).
- [22] <https://www.gfdl.noaa.gov/coupled-physical-model-cm3/>
- [23] <https://www.metoffice.gov.uk/research/modelling-systems/unified-model/climate-models/hadgem2>
- [24] <https://www.mpimet.mpg.de/en/science/models/mpi-esm/>
- [25] E. Kostopoulou, C. Giannakopoulos, C. Anagnostopoulou, K. Tolika, P. Maheras, M. Vafiadis, D. Founda, Simulating maximum and minimum temperature over Greece: a comparison of three downscaling techniques. *Theoretical and Applied Climatology* 90 (2007) 65–82. DOI: 10.1007/s00704-006-0269-x.
- [26] MK. Goyal, CSP. Ojha, Evaluation of linear regression methods as downscaling tools in temperature projections over the Pichola Lake Basin in India. *Hydrol Processes* 25 (2011) 1453–1465.
- [27] E. Hawkins, T.M. Osborne, Ch. Kit Ho, A.J. Challinor, Calibration and bias correction of climate projections for crop modelling: An idealised case study over Europe. *Agricultural and Forest Meteorology*, 170 (2013) 19–31.
- [28] RE. Benestad, D. Chen, A. Mezghani, L. Fan, K. Parding, On using principal components to represent stations in empirical–statistical downscaling. *Tellus A* 67 (2015) 1–11.
- [29] MK. Goyal, CSP. Ojha, Downscaling of surface temperature for lake catchment in an arid region in India using linear multiple regression and neural networks. *Int J Climatol* 32 (2012) 552–566.
- [30] <http://r-instat.org/>
- [31] J.R. Lanzante, Resistant, Robust and Non-Parametric Techniques for the Analysis of Climate Data: Theory and Examples, including Applications to Historical Radiosonde Station Data. *International Journal of Climatology* 16 (1996) 1197–1226. [http://dx.doi.org/10.1002/\(SICI\)1097-0088\(199611\)16:11<1197::AID-JOC89>3.0.CO;2-L](http://dx.doi.org/10.1002/(SICI)1097-0088(199611)16:11<1197::AID-JOC89>3.0.CO;2-L)
- [32] Y. B. Dibike, P. Gachon, A. St-Hilaire, T. B. M. J. Ouarda, and Van T.-V. Nguyen. Uncertainty analysis of statistically downscaled temperature and precipitation regimes in Northern Canada. *Theor. Appl. Climatol.* 91, 149–170 (2008) DOI 10.1007/s00704-007-0299-z

Appendices

Appendix A: Figures

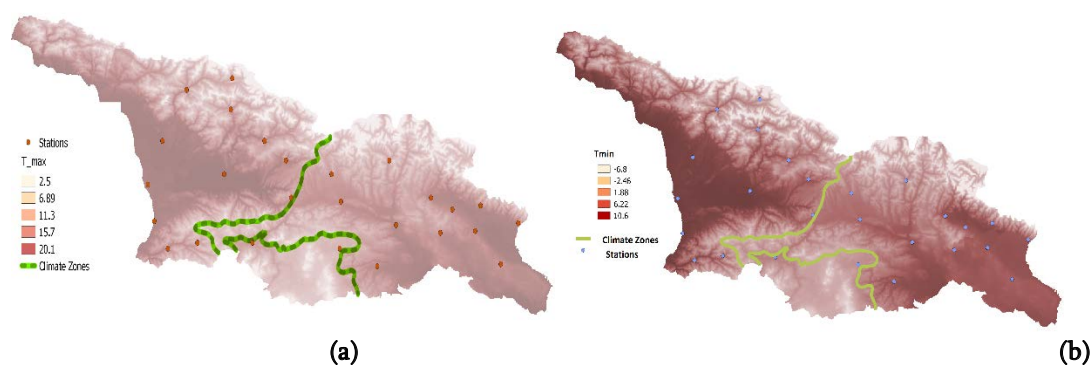


Fig. A.1 Maps of annual mean maximal (a) and minimal (b) temperatures for 1961-85 period, interpolated from observation of 90 Georgian meteorological network's stations.

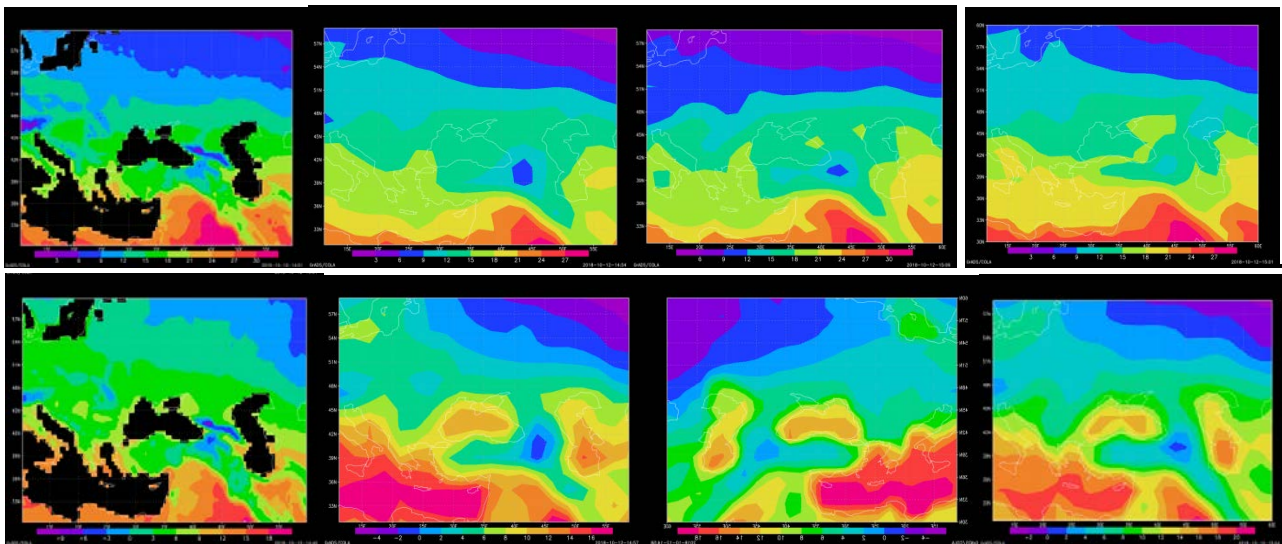


Fig. A.2. Maps of observed and simulated Tmax and Tmin for 1961-85 period. The first plot on the upper panel is Tmax constructed from CRU data, the second – from the output of GFDL-CM3, III and IV – from HadGEM2-ES and MPI-ESM-MR, respectively. On the second panel are identical maps for Tmin.

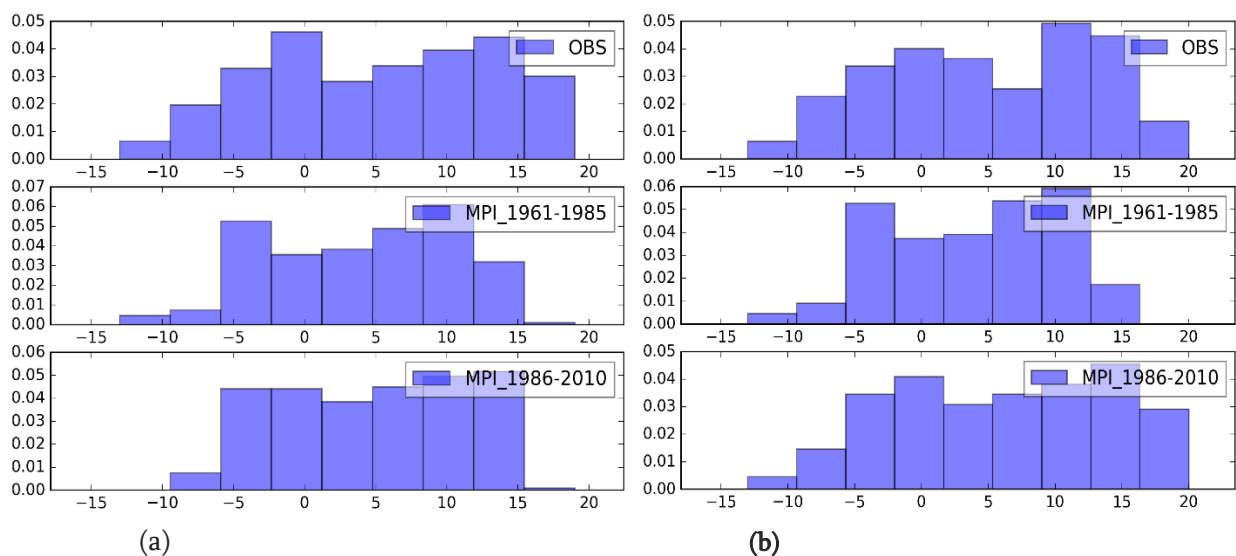


Fig. A.3 (a) Original and (b) downsampled by delta addition method mean Tmin time series frequency distribution of observed and MPI simulated ones for two periods for Tbilisi.

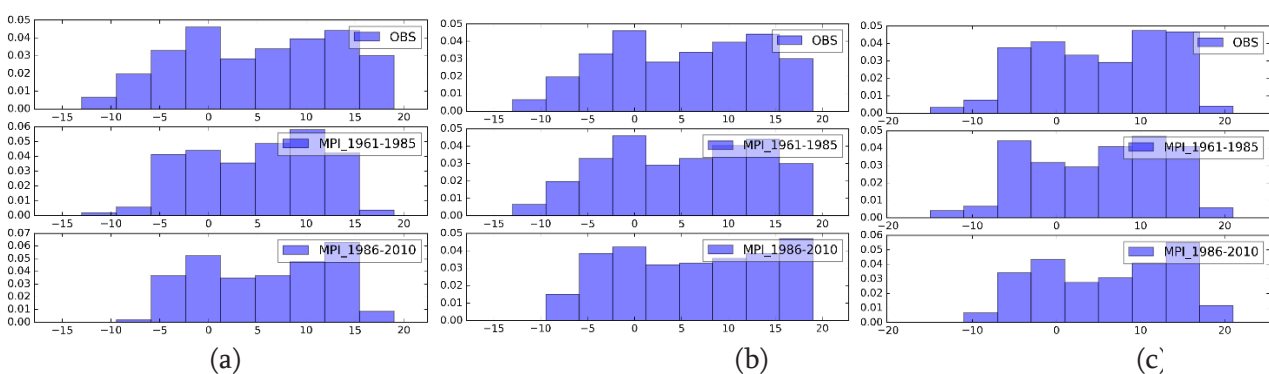


Fig. A.4. Frequency distribution of mean Tmin time series for two periods for Tbilisi observed and MPI simulated downscaled by (a) Delta method (bias correction); (b) quartile mapping; (c) Statistical Asynchronous Regression (SAR) method.

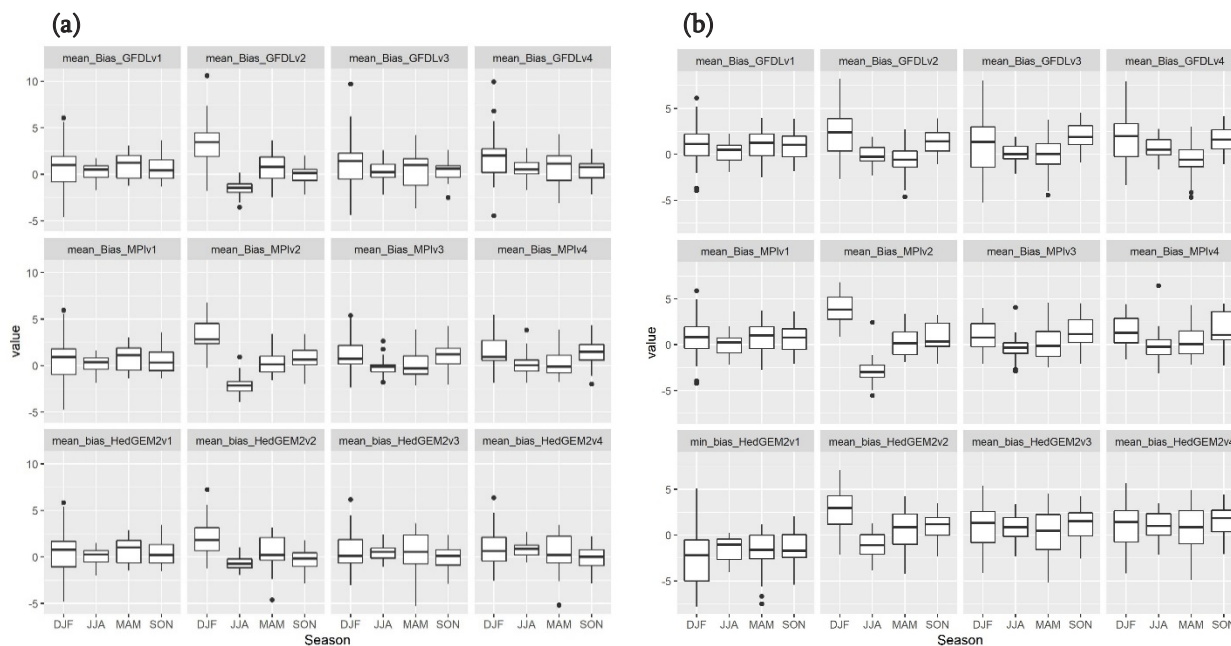


Fig. A.5. Mean bias values by seasons between the observed and downscaled projections of mean monthly minimum (a) and maximum (b) temperatures at 27 stations in Georgia for validation period (1986-2010). Downscaling methods are shown as: 1 – Delta Addition, 2 – Delta Correction, 3 – Quantile Mapping, 4 – Asynchronous Linear Regression. Solid lines show medians, the boxes represent the range between first and third quartiles, and the whiskers indicate minimum and maximum values of all data.

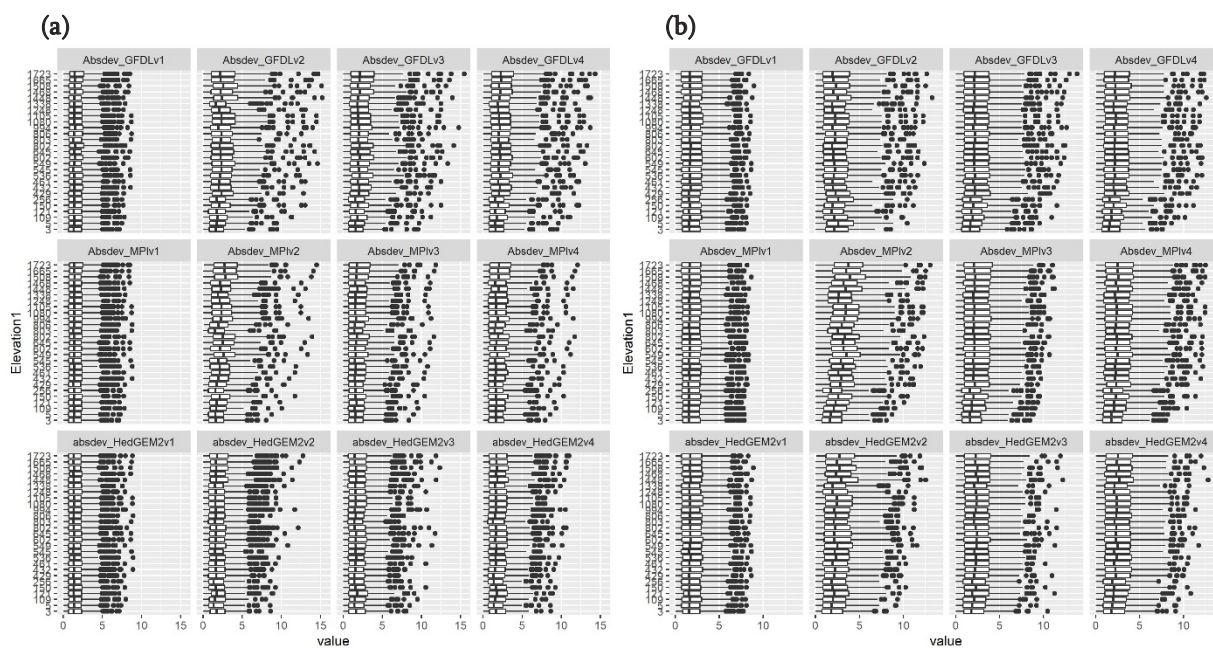


Fig. A.6. Mean Absolute Errors (MAE) between the observed and downscaled projections of mean monthly minimum (a) and maximum (b) temperatures at 27 stations in Georgia for validation period (1986-2010). Values are plotted as a function of the station elevations. Downscaling methods are shown as: 1 – Delta Addition, 2 – Delta Correction, 3 – Quantile Mapping, 4 – Asynchronous Linear Regression. Solid lines show medians, the boxes represent the range between first and third quartiles, and the whiskers indicate minimum and maximum values of all data.

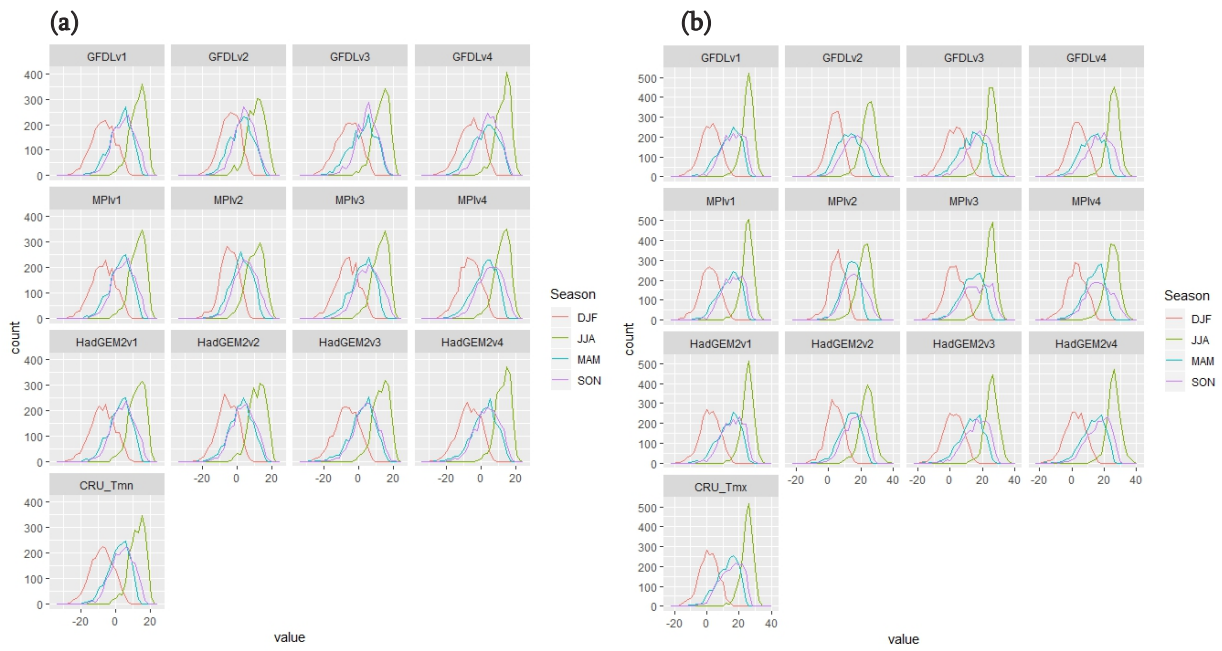


Fig. A.7. Frequency polygons by seasons for the observed and downscaled projections of mean monthly minimum (a) and maximum (b) temperatures at 27 stations in Georgia for validation period (1986-2010). Downscaling methods are shown as: 1 – Delta Addition, 2 – Delta Correction, 3 – Quantile Mapping, 4 – Asynchronous Linear Regression.

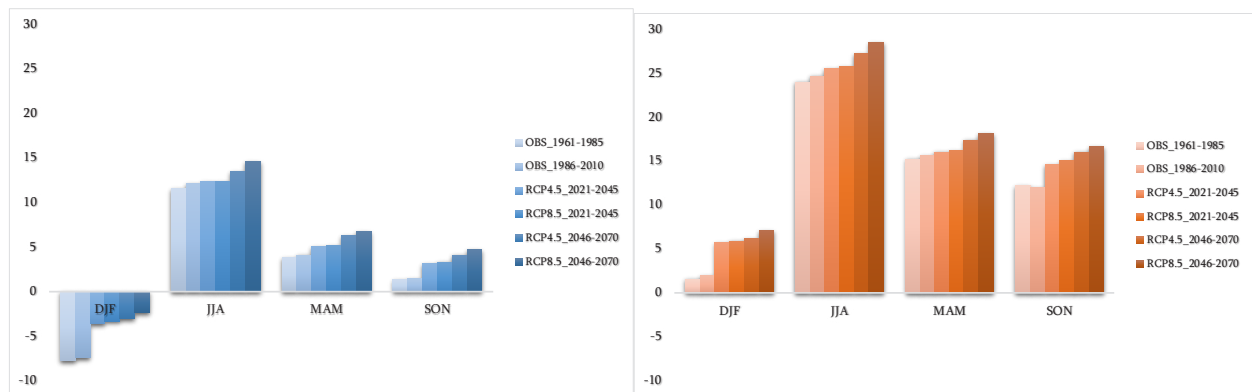
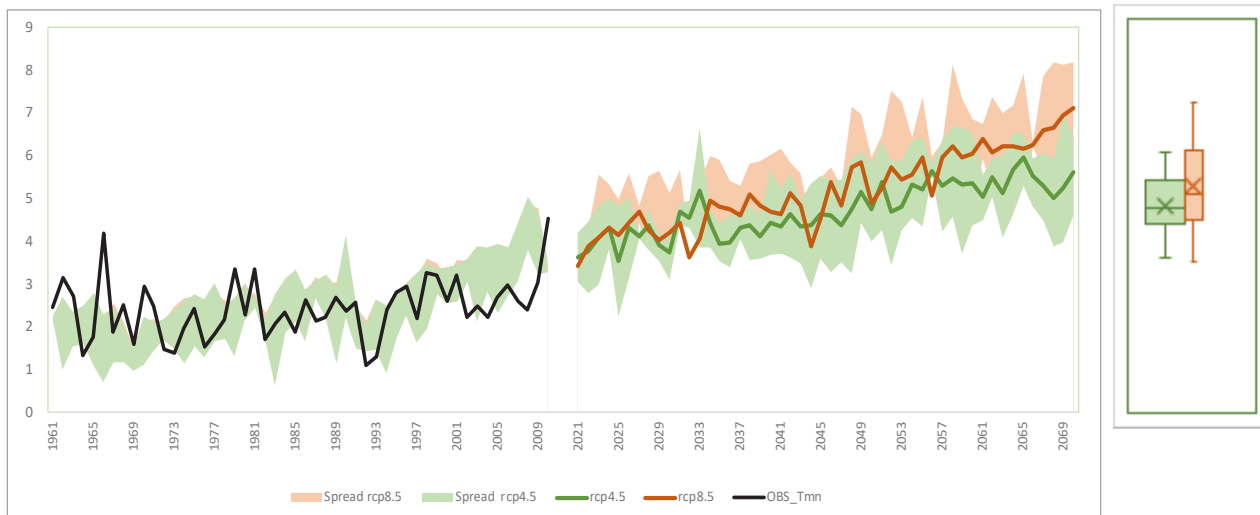


Fig. A.8. Mean seasonal observed and projected minimum (a) and maximum (b) temperatures under RCP4.5 and RCP8.5 scenarios simulated by the subset of CMIP5 multi-model ensemble presented for four 25-years periods.

(a)



(b)

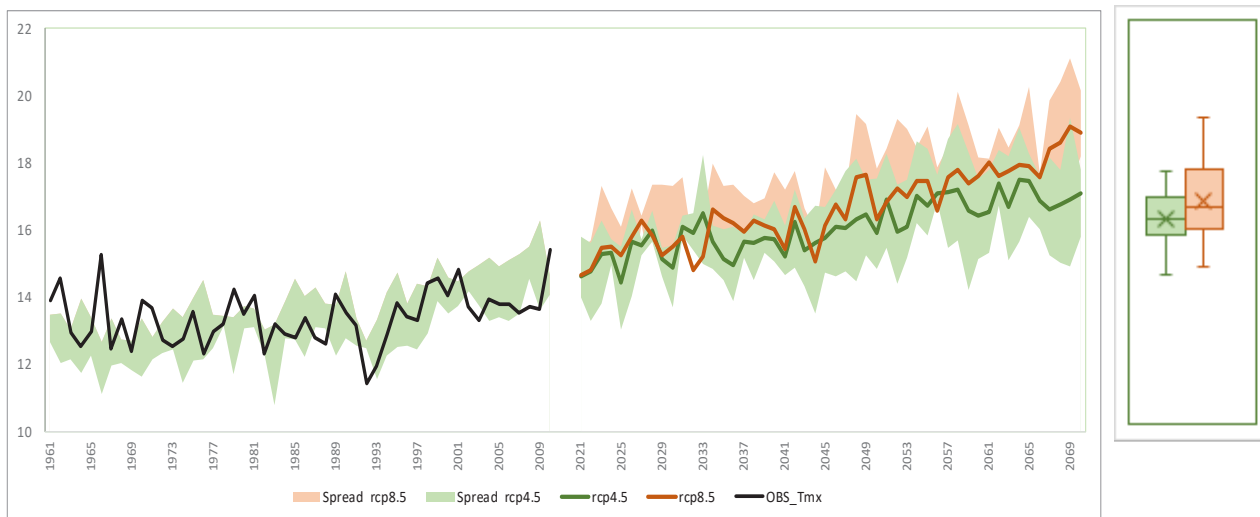


Fig. A. 9 Time series of historical and projected change for the mean annual minimum (a) and maximum (b) temperatures, as simulated by the subset of CMIP5 multi-model ensemble averaged over 27 stations of Georgia. The shaded areas represent the spread of simulation results for individual models, while the heavy lines indicate the ensemble average. Results are based on statistical downscaling of 27 weather stations in Georgia. Change is computed relative to the 1961-2010 period. The spread amongst models, evident from the shaded area, is quantified by the box and whisker plots to the right of each panel. The boxes represent the range between first and third quartiles, and the whiskers indicate minimum and maximum values of all data for the 2021-2070 period for RCP4.5 and RCP8.5 scenarios separately.

Appendix B. Tables

Table B.2. Summary information for the selected stations in Georgia

| # | Station Name | Elevation (m) | Latitude (°N) | Longitude (°E) |
|----|----------------|------------------|------------------|-------------------|
| 1 | Akhalqalaqi | 1723 | 41.40 | 43.48 |
| 2 | Akhaltzikhe | 994 | 41.65 | 43.00 |
| 3 | Ambrolauri | 549 | 42.53 | 43.13 |
| 4 | Bakuriani | 1665 | 41.73 | 43.52 |
| 5 | Bolnisi | 536 | 41.45 | 44.57 |
| 6 | Borjomi | 802 | 41.83 | 43.38 |
| 7 | Dedoplistskaro | 803 | 41.47 | 46.10 |
| 8 | Gori | 602 | 42.00 | 44.12 |
| 9 | Khashuri | 645 | 42.03 | 43.82 |
| 10 | Khulo | 1338 | 41.65 | 42.30 |
| 11 | Lagodekhi | 429 | 41.82 | 46.30 |
| 12 | Mestia | 1448 | 43.07 | 42.75 |
| 13 | Mta-Sabueti | 1248 | 42.03 | 43.47 |
| 14 | Pasanauri | 1080 | 42.35 | 44.68 |
| 15 | Poti | 3 | 42.13 | 41.68 |
| 16 | Qeda | 256 | 41.60 | 41.92 |
| 17 | Qobuleti | 5 | 41.87 | 41.78 |
| 18 | Qutaisi | 109 | 42.25 | 42.62 |
| 19 | Sachkhere | 461 | 42.33 | 43.43 |
| 20 | Sagarejo | 806 | 41.75 | 45.32 |
| 21 | Shovi | 1508 | 42.70 | 43.68 |
| 22 | Tbilisi | 432 | 41.75 | 44.77 |
| 23 | Telavi | 545 | 41.93 | 45.52 |
| 24 | Tianeti | 1105 | 42.10 | 44.97 |
| 25 | Tsalka | 1468 | 41.60 | 44.10 |
| 26 | Zestaphoni | 150 | 42.12 | 43.02 |
| 27 | Zugdidi | 121 | 42.52 | 41.88 |

Table B.3. Explained variances between candidate methods of mean minimum (a) and maximum (b) temperatures (predicted) over the Georgia territory. Values are Pearson’s correlation coefficients (CC) averaged over 27 weather stations (Table 1). Downscaling methods are shown as: 1 – Delta Addition, 2 – Delta Correction, 3 – Quantile Mapping, 4 – Asynchronous Linear Regression

(a)

| GCM | | GFDL | | | | MPI | | | | HadGEM2 | | | |
|--------|-----|------|------|------|------|------|------|------|------|---------|------|------|------|
| Method | | 1 | 2 | 3 | 4 | 1 | 2 | 3 | 4 | 1 | 2 | 3 | 4 |
| Season | DJF | 0.91 | 0.88 | 0.88 | 0.87 | 0.91 | 0.96 | 0.96 | 0.97 | 0.91 | 0.90 | 0.90 | 0.90 |
| | MA | | | | | | | | | | | | |
| | M | 0.96 | 0.94 | 0.91 | 0.91 | 0.96 | 0.96 | 0.94 | 0.94 | 0.96 | 0.92 | 0.90 | 0.91 |
| | JJA | 0.98 | 0.96 | 0.96 | 0.96 | 0.98 | 0.96 | 0.97 | 0.95 | 0.97 | 0.96 | 0.95 | 0.95 |
| | SON | 0.96 | 0.97 | 0.96 | 0.96 | 0.96 | 0.97 | 0.95 | 0.95 | 0.96 | 0.97 | 0.96 | 0.96 |

(b)

| GCM | | GFDL | | | | MPI | | | | HadGEM2 | | | |
|--------|-----|------|------|------|------|------|------|------|------|---------|------|------|------|
| Method | | 1 | 2 | 3 | 4 | 1 | 2 | 3 | 4 | 1 | 2 | 3 | 4 |
| Season | DJF | 0.88 | 0.85 | 0.84 | 0.88 | 0.88 | 0.96 | 0.96 | 0.96 | 0.88 | 0.87 | 0.89 | 0.88 |
| | MA | | | | | | | | | | | | |
| | M | 0.91 | 0.88 | 0.86 | 0.87 | 0.91 | 0.92 | 0.88 | 0.89 | 0.91 | 0.85 | 0.83 | 0.81 |
| | JJA | 0.93 | 0.88 | 0.92 | 0.90 | 0.93 | 0.86 | 0.88 | 0.82 | 0.92 | 0.91 | 0.87 | 0.86 |
| | SON | 0.91 | 0.93 | 0.91 | 0.91 | 0.92 | 0.92 | 0.90 | 0.88 | 0.91 | 0.92 | 0.89 | 0.89 |

Table B.4. Statistical comparison of observed and downscaled mean monthly minimum (a) and maximum (b) temperatures during validation period (1986-2010). Downscaling methods are shown as: 1 – Delta Addition, 2 – Delta Correction, 3 – Quantile Mapping, 4 – Asynchronous Linear Regression

(a)

| Method | Model | μ | Med | SE $_{\mu}$ | SD | CV | MAD | Bias | MAE | RMSE |
|--------|---------|-------|------|-------------|------|------|------|------|------|------|
| 1 | CRU | 2.58 | 3.20 | 0.17 | 8.74 | 3.39 | 8.40 | | | |
| | GFDL | 3.22 | 4.00 | 0.17 | 8.59 | 2.67 | 8.18 | 0.65 | 1.33 | 1.73 |
| | MPI | 3.12 | 3.91 | 0.17 | 8.59 | 2.76 | 8.13 | 0.54 | 1.30 | 1.69 |
| | HedGEM2 | 2.99 | 3.83 | 0.17 | 8.63 | 2.88 | 8.20 | 0.33 | 1.30 | 1.70 |
| 2 | GFDL | 3.22 | 3.52 | 0.14 | 7.31 | 2.27 | 7.43 | 0.65 | 2.00 | 2.72 |
| | MPI | 3.12 | 3.46 | 0.14 | 7.19 | 2.31 | 7.42 | 0.54 | 1.98 | 2.53 |
| | HedGEM2 | 2.99 | 3.21 | 0.15 | 7.91 | 2.64 | 8.28 | 0.33 | 1.62 | 2.19 |
| 3 | GFDL | 3.23 | 3.83 | 0.16 | 8.49 | 2.63 | 8.43 | 0.66 | 1.60 | 2.20 |
| | MPI | 3.13 | 3.78 | 0.16 | 8.42 | 2.69 | 8.50 | 0.55 | 1.35 | 1.76 |
| | HedGEM2 | 3.00 | 3.38 | 0.17 | 8.71 | 2.90 | 8.63 | 0.33 | 1.44 | 1.93 |
| 4 | GFDL | 3.52 | 4.05 | 0.16 | 8.37 | 2.38 | 8.55 | 0.94 | 1.68 | 2.32 |
| | MPI | 3.41 | 4.00 | 0.16 | 8.32 | 2.44 | 8.70 | 0.84 | 1.47 | 1.90 |
| | HedGEM2 | 3.16 | 3.39 | 0.17 | 8.66 | 2.75 | 9.07 | 0.48 | 1.53 | 2.03 |

(b)

| Method | Model | μ | Med | SE $_{\mu}$ | SD | CV | MAD | Bias | MAE | RMSE |
|--------|---------|-------|-------|-------------|------|------|-------|------|------|------|
| 1 | CRU | 13.56 | 14.73 | 0.18 | 9.42 | 0.69 | 9.34 | | | |
| | GFDL | 14.32 | 15.49 | 0.18 | 9.26 | 0.65 | 9.00 | 0.76 | 1.58 | 1.98 |
| | MPI | 14.06 | 15.22 | 0.18 | 9.27 | 0.66 | 9.09 | 0.50 | 1.50 | 1.89 |
| 2 | HedGEM2 | 14.33 | 15.54 | 0.18 | 9.27 | 0.65 | 9.03 | 0.77 | 1.58 | 1.98 |
| | GFDL | 14.32 | 14.78 | 0.17 | 8.76 | 0.61 | 9.76 | 0.76 | 1.96 | 2.54 |
| | MPI | 14.06 | 14.64 | 0.14 | 7.32 | 0.52 | 7.53 | 0.50 | 2.44 | 3.02 |
| 3 | HedGEM2 | 14.33 | 14.90 | 0.16 | 8.27 | 0.58 | 8.45 | 0.77 | 2.03 | 2.55 |
| | GFDL | 14.34 | 15.68 | 0.18 | 9.33 | 0.65 | 9.78 | 0.77 | 1.86 | 2.41 |
| | MPI | 14.07 | 15.14 | 0.17 | 9.09 | 0.65 | 9.63 | 0.51 | 1.55 | 1.96 |
| 4 | HedGEM2 | 14.34 | 15.35 | 0.18 | 9.55 | 0.67 | 9.86 | 0.78 | 1.86 | 2.26 |
| | GFDL | 14.45 | 15.26 | 0.18 | 9.19 | 0.64 | 10.00 | 0.89 | 1.84 | 2.39 |
| | MPI | 14.38 | 15.35 | 0.17 | 9.02 | 0.63 | 9.35 | 0.81 | 1.71 | 2.19 |
| | HedGEM2 | 14.60 | 15.66 | 0.18 | 9.54 | 0.65 | 9.65 | 1.04 | 1.96 | 2.38 |

Table B.5. Statistical trends slope and significance of observed and downscaled mean monthly minimum (a) and maximum (b) temperatures during validation period (1986-2010). Downscaling methods are shown as: 1 – Delta Addition, 2 – Delta Correction, 3 – Quantile Mapping, 4 – Asynchronous Linear Regression

(a)

| Model | GFDL | | | | MPI | | | | HadGEM2 | | | | CRU | | |
|-------|------|------|------|------|------|------|------|------|---------|------|------|------|------|-------|-------|
| | 1 | 2 | 3 | 4 | 1 | 2 | 3 | 4 | 1 | 2 | 3 | 4 | | | |
| Slope | DJF | - | 0.01 | 0.02 | 0.02 | - | 0.00 | 0.01 | 0.00 | - | 0.08 | 0.09 | 0.09 | - | |
| | | 0.00 | 8 | 9 | 7 | 4 | 0.00 | 8 | 7 | 8 | 9 | 8 | 6 | 8 | 9 |
| | MAM | 0.00 | 0.08 | 0.10 | 0.10 | 0.00 | 0.05 | 0.07 | 0.07 | 0.00 | 0.08 | 0.10 | 0.10 | | |
| | | 3 | 4 | 7 | 4 | 3 | 7 | 8 | 2 | 3 | 8 | 9 | 1 | 0.043 | |
| | JJA | - | 0.03 | 0.05 | 0.07 | 0.07 | - | 0.03 | 0.07 | 0.07 | 0.08 | 0.03 | 0.06 | 0.08 | 0.07 |
| | | 0 | 8 | 2 | 2 | 0 | 0 | 1 | 9 | 0 | 1 | 0 | 0 | 0.040 | |
| | SON | - | 0.00 | 0.05 | 0.06 | 0.06 | - | 0.00 | 0.10 | 0.11 | 0.12 | - | 0.07 | 0.08 | 0.08 |
| | | 8 | 1 | 4 | 2 | 8 | 0 | 9 | 7 | 8 | 4 | 5 | 5 | 0.066 | |
| | Rho | DJF | 0.00 | 0.12 | 0.17 | 0.12 | 0.00 | 0.06 | 0.12 | 0.06 | 0.00 | 0.23 | 0.23 | 0.22 | - |
| | | | 9 | 9 | 8 | 5 | 9 | 7 | 8 | 7 | 9 | 5 | 0 | 2 | 0.080 |
| | | MAM | 0.00 | 0.36 | 0.37 | 0.36 | 0.00 | 0.41 | 0.38 | 0.41 | 0.00 | 0.45 | 0.50 | 0.45 | |
| | | | 6 | 1 | 5 | 1 | 6 | 1 | 2 | 1 | 6 | 9 | 5 | 8 | 0.339 |
| JJA | | - | 0.32 | 0.47 | 0.43 | 0.45 | - | 0.32 | 0.53 | 0.53 | 0.53 | 0.32 | 0.68 | 0.70 | 0.68 |
| | | 2 | 2 | 2 | 5 | 2 | 5 | 6 | 6 | 2 | 7 | 5 | 7 | 0.380 | |
| SON | | - | 0.03 | 0.40 | 0.42 | 0.40 | - | 0.03 | 0.64 | 0.61 | 0.64 | 0.03 | 0.55 | 0.54 | 0.55 |
| | | 5 | 0 | 8 | 9 | 5 | 5 | 2 | 4 | 5 | 8 | 4 | 5 | 0.603 | |

(b)

| Model | | GFDL | | | | MPI | | | | HadGEM2 | | | | CRU | | | | |
|------------------|-----|------|------|------|------|------|------|------|------|---------|------|------|------|------|------|-------|-------|-------|
| Method | | 1 | 2 | 3 | 4 | 1 | 2 | 3 | 4 | 1 | 2 | 3 | 4 | | | | | |
| S _{10m} | DJF | - | 0.03 | 0.01 | 0.02 | 0.01 | - | 0.03 | 0.00 | 0.00 | 0.00 | - | 0.03 | 0.09 | 0.10 | 0.11 | 0.035 | |
| | | | 9 | 6 | 1 | 7 | | 9 | 5 | 6 | 6 | | 9 | 5 | 3 | 3 | | |
| | MAM | - | 0.01 | 0.09 | 0.11 | 0.10 | - | 0.01 | 0.05 | 0.07 | 0.06 | - | 0.01 | 0.09 | 0.11 | 0.11 | | 0.050 |
| | | | 5 | 9 | 4 | 4 | | 5 | 1 | 4 | 6 | | 5 | 8 | 9 | 7 | | |
| JJA | - | 0.01 | 0.07 | 0.07 | 0.08 | - | 0.01 | 0.08 | 0.08 | 0.11 | - | 0.01 | 0.07 | 0.09 | 0.09 | 0.047 | | |
| | | 0 | 8 | 2 | 2 | | 0 | 4 | 0 | 0 | | 0 | 6 | 6 | 1 | | | |
| SON | - | 0.01 | 0.07 | 0.07 | 0.08 | - | 0.01 | 0.10 | 0.12 | 0.13 | - | 0.01 | 0.05 | 0.07 | 0.06 | | 0.076 | |
| | | 6 | 8 | 9 | 2 | | 6 | 3 | 5 | 4 | | 6 | 7 | 0 | 8 | | | |
| DJF | - | 0.15 | 0.11 | 0.11 | 0.11 | - | 0.15 | 0.05 | 0.06 | 0.05 | - | 0.15 | 0.28 | 0.27 | 0.28 | 0.122 | | |
| | | 8 | 4 | 9 | 4 | | 8 | 5 | 4 | 5 | | 8 | 8 | 4 | 8 | | | |
| MAM | - | 0.08 | 0.32 | 0.31 | 0.32 | - | 0.08 | 0.22 | 0.20 | 0.22 | - | 0.08 | 0.37 | 0.39 | 0.37 | | 0.372 | |
| | | 7 | 1 | 8 | 1 | | 7 | 8 | 8 | 3 | | 7 | 5 | 0 | 6 | | | |
| JJA | - | 0.11 | 0.42 | 0.42 | 0.42 | - | 0.11 | 0.42 | 0.45 | 0.42 | - | 0.11 | 0.36 | 0.43 | 0.36 | 0.382 | | |
| | | 8 | 1 | 8 | 1 | | 8 | 4 | 0 | 4 | | 8 | 6 | 5 | 3 | | | |
| SON | - | 0.13 | 0.40 | 0.40 | 0.39 | - | 0.13 | 0.47 | 0.47 | 0.47 | - | 0.13 | 0.36 | 0.29 | 0.36 | | 0.589 | |
| | | 8 | 2 | 0 | 7 | | 8 | 2 | 2 | 2 | | 8 | 3 | 8 | 3 | | | |

Table B. 6. Mean seasonal changes in observed and projected minimum (a) and maximum (b) temperatures under RCP4.5 and RCP8.5 scenarios simulated by the subset of CMIP5 multi-model ensemble between four 25-years periods. Differences are shown as: Δ , indexes indicate comparable periods, corresponding to: 1 - 1961–1985, 2 - 1986–2010, 3 – 2021–2045, 4 – 2046–2070

| | Season | Δ_{21_OBS} | $\Delta_{32_RCP4.5}$ | $\Delta_{32_RCP8.5}$ | $\Delta_{42_RCP4.5}$ | $\Delta_{42_RCP8.5}$ |
|--------------------------|--------|--------------------|-----------------------|-----------------------|-----------------------|-----------------------|
| T _{min} , °C | DJF | 0.32 | 3.82 | 4.12 | 4.36 | 5.09 |
| | JJA | 0.60 | 0.15 | 0.14 | 1.28 | 2.37 |
| | MAM | 0.27 | 1.01 | 1.12 | 2.15 | 2.62 |
| | SON | 0.08 | 1.65 | 1.90 | 2.67 | 3.30 |
| | Year | 0.32 | 1.66 | 1.82 | 2.62 | 3.35 |
| T _{max} , °C | DJF | 0.40 | 3.73 | 3.99 | 4.29 | 5.19 |
| | JJA | 0.69 | 0.90 | 1.03 | 2.53 | 3.80 |
| | MAM | 0.34 | 0.41 | 0.56 | 1.80 | 2.46 |
| | SON | -0.13 | 2.60 | 3.05 | 3.96 | 4.58 |
| | Year | 0.32 | 1.91 | 2.15 | 3.14 | 4.01 |